

Engulfment and Cell Motility¹ Regulate Tumor Cell Behaviors and Predict Prognosis in Colorectal Cancer

Young-Lan Park

Chosun University

Sung-Bum Cho

Chonnam National University Medical School

Sun-Young Park

Chonnam National University Medical School

Hyung-Hoon Oh

Chonnam National University Medical School

Eun Myung

Chonnam National University Medical School

Chan-Muk Im

Chonnam National University Medical School

Seyeong Son

Chonnam National University Medical School

Seunghee Kim

Chonnam National University Medical School

Seo-Yeon Cho

Chonnam National University Medical School

Min-Woo Chung

Chonnam National University Medical School

Ji-Yun Hong

Chonnam National University Medical School

Ki-Hyun Kim

Chonnam National University Medical School

Dae-Seong Myung

Chonnam National University Medical School

Wan-Sik Lee

Chonnam National University Medical School

Daeho Park

Gwangju Institute of Science and Technology

Young-Eun Joo (✉ yejoo@chonnam.ac.kr)

Research Article

Keywords: ELM01, Oncogenic phenotype, Prognosis, Tumor progression, Colorectal neoplasm

Posted Date: February 25th, 2022

DOI: <https://doi.org/10.21203/rs.3.rs-1356572/v1>

License:  This work is licensed under a Creative Commons Attribution 4.0 International License.

[Read Full License](#)

Abstract

Background: Engulfment and cell motility 1 (ELMO1) plays a crucial role in the process of migration, chemotaxis, and metastasis of tumor cells. ELMO 1 has been implicated in the pathogenesis of various cancers. However, the distinct function of ELMO1 in colorectal cancer (CRC) is unclear. We determined whether ELMO1 affected the oncogenic behavior of CRC cells and investigated its prognostic value in CRC patients.

Methods: We investigated the impact of ELMO1 on tumor cell behaviors using small interference RNA in CRC cell lines, including SW480 and DLD1. The expression of ELMO1 was investigated by reverse transcription-polymerase chain reaction, immunohistochemistry, and enzyme-linked immunosorbent assay in cancer tissues and sera taken from CRC patients.

Results: ELMO1 knockdown suppressed tumor cell proliferation in SW480 and DLD1 cells. ELMO1 knockdown-induced apoptosis through up-regulation of caspase-3, -7, and PARP activities and down-regulation of the anti-apoptotic Mcl-1 protein. ELMO1 knockdown-induced cell cycle arrest by decreasing cyclin D1, cyclin-dependent kinase 2, 4 and 6, and the 25C cell division cycle (CDC25C). ELMO1 knockdown suppressed tumor cell invasion and migration. The expression of E-cadherin was increased, and Vimentin and Claudin 1 decreased with ELMO1 knockdown. The phosphorylation levels of PDK1, Akt, and GSK-3 β and were down-regulated by ELMO1 knockdown. The expression of ELMO1 was up-regulated in cancer tissues and sera taken from CRC patients. ELMO1 expression was significantly associated with tumor stage, lymph node metastasis, distant metastases, and poor survival.

Conclusions: These results indicate that ELMO1 mediates tumor progression by increasing tumor cell motility and inhibiting apoptosis in human CRC.

Introduction

Colorectal cancer (CRC) is one of the major causes of cancer-associated morbidity and mortality worldwide. In recent years, the survival of CRC patients has improved dramatically through early diagnosis and the development of newer therapeutic drugs. The 5-year survival rate for CRC patients in the early stage is 80–90%, while the 5-year survival rate for patients in the advanced stage is less than 40% [1, 2]. Therefore, identifying biomarkers that can detect CRC early or monitor cancer progression and the development of novel targets enable us to improve the survival rates of CRC patients (3, 4). The underlying molecular mechanisms that can contribute to the development and progression of CRC include inhibition of tumor cell apoptosis, enhancement of tumor cell proliferation, stimulation of epithelial-mesenchymal transition (EMT), and inhibition of immune escape (5–7).

The Engulfment and Cell Motility (ELMO) protein family is an evolutionarily conserved cytoplasmic engulfment protein and binds to the dedicator of cytokinesis 180 (DOCK180), a guanine nucleotide exchange factor (GEF) of the Ras-related C3 botulinum toxin substrate family (Rac), and regulates GEF activity (8–11). The resultant ELMO / DOCK180 module promotes Rac-dependent actin cytoskeletal

reorganization responsible for the engulfment of apoptotic cells, cell migration, neurite outgrowth, and chemotaxis. In mammals, the ELMO protein family consists of 3 members: ELMO1, ELMO2, and ELMO3 (12–15). ELMO1 and ELMO2 have been shown to function identically in remodeling of the cytoskeleton during cell migration, phagocytosis, and chemotaxis (12–15). However, the function of ELMO3 is not yet fully understood.

Recently, ELMO has also been pivotal for proliferation, adhesion to the extracellular matrix, EMT, migration, invasion, and metastasis of cancer cells (16–19). ELMO1 is aberrantly expressed in various human malignant tumors, including hepatocellular carcinoma, ovarian cancer, glioma, breast cancer, acute myeloid leukemia, and gastric cancer. It is closely related to tumor progression and prognosis (20–25). Furthermore, ELMO3 expression is involved in the processes of tumor growth, invasion and metastasis of colorectal cancer, gastric cancer, and nonsmall cell lung cancer (26–28). However, the distinct function of ELMO1 in CRC has not yet been explored.

The objectives of the current study were to evaluate whether ELMO1 affects the oncogenic biologic behaviors of human CRC cells, evaluate the expression of ELMO1 in human CRC tissues, and examine the relationship of its correlation with various clinicopathological characteristics, including survival.

Materials And Methods

Cell culture and siRNA transfection

DKO1, COLO205, HCT116, SW480 and DLD1 cells (human CRC cell lines) cells were obtained from the American Type Culture Collection (Masassa, VA, USA) and cultured in Dulbecco's modified Eagle medium (DMEM; Gibco, Thermo Fisher Scientific, Inc., Waltham, MA, USA) supplemented with 10% fetal bovine serum (FBS), 100 U / ml penicillin, 100 µg/mL streptomycin and 50 µg/mL gentamycin; Gibco, Thermo Fisher Scientific, Inc.). Cultures were kept at 37°C with 5% CO₂ in a humidified atmosphere. Small interfering (si)RNA (5'- GACAUGAUGAGCGACCUGA-dTdT -3') and scrambled control used as negative control siRNA (cat. No. #SN-1002) were purchased from Bioneer (Daejeon, Korea). Transfection of the siRNA was performed using Lipofectamin™ RNAiMAX (Invitrogen, Thermo Fisher Scientific, Inc. Waltham, MA, USA), according to the manufacturer's protocol. Briefly, SW480 and DLD1 cells were seeded into 6-well plates such that they would be 40-60% confluent at the time of transfection. 100 µM of ELMO1 siRNA and negative control siRNA was transfected with 5 µL Lipofectamine™ RNAiMAX reagent (Invitrogen; Thermo Fisher Scientific, Inc.), respectively. After incubation for 48 hours at 37°C, identification of ELMO1 expression was performed by western blotting and transfected cells and siRNA-transfected cells were applied to each experiment.

Cell proliferation assay

The effects of ELMO1 siRNA on cell proliferation in SW480 and DLD1 cells were determined by the water-soluble tetrazolium salts (WST)-1 assay (Daeil lab Inc., Seoul, South Korea) assay. In summary, cells were dispersed within culture plates. 10% WST-1 reagent was added to each well 1 hour before the end of

incubation. The optical density (OD) values at 450 nm in each well were determined by a microplate reader (Infinite M200; Tecan, Austria GmbH, Austria). Each experiments were performed in triplicate wells and were repeated at least thrice.

Western blotting

Total protein extracts were prepared using RIPA[®] reagent (Thermo, Rockford, IL, USA) containing protease and phosphatase inhibitors. Protein quantification of each sample was performed using the BCA[™] protein assay (Thermo, Rockford, IL, USA). Subsequently, total protein samples were subjected to 8~12% SDS-PAGE and transferred to polyvinylidene fluoride membranes (PVDF, Millipore, Billerica, MA, USA). The blots were blocked with 5% BSA at room temperature and incubated overnight at 4 ° C with primary antibodies at 1: 1000 dilution. The blots were then washed with Tris-buffered saline / 0.1% Tween-20 and incubated with horseradish peroxidase (HRP) conjugated secondary antibody (Cell Signaling, Danvers, MA, USA) at a dilution of 1: 2000. Protein bands were visualized using a chemiluminescent HRP substrate (Millipore, Billerica, MA, USA) and the LAS-4000 luminescent image analyzer (Fujifilm, Tokyo, Japan). Immunoblots were quantified using Multi-Gauge gel analysis software (ver 3.0, Fujifilm, Tokyo, Japan). Antibody against ELMO1 and GAPDH was purchased from Abcam (cat. No. ab2239, Cambridge, UK) and Santa Cruz Biotechnology (cat. No. FL-335, Santa Cruz, CA, USA), respectively. Antibodies against cleaved caspase-3 (cat. No. #9664), cleaved caspase-7 (cat. No. #8438), cleaved poly (ADP-ribose) polymerase (PARP, cat. No. #5625), Mcl-1 (cat. No. #2453), cyclin-dependent kinase (CDK) 2 (cat. No. #2546), CDK4 (cat. No. #2906), CDK6 (cat. No. #3136), Cyclin D1 (cat. No. #2926), cell division cycle (CDC) 25C (cat. No. #4688), phospho-Akt (cat. No. #4060), phospho-glycogen synthase kinase-3 β (phospho-GSK3 β , cat. No. #5558), phospho-phosphoinositide-dependent protein kinase 1 (phospho-PDK1, cat. No. #3438), E-cadherin (cat. No. #3195), Vimentin (cat. No. #5741), Claudin1 (cat. No. #13255) were purchased from Cell Signaling (Danvers, MA, USA). All experiments were repeated at least 3 times and bands of immunoblot were quantified using Multi-Gauge software (ver 3.0, Fujifilm, Tokyo, Japan).

Analysis of apoptosis by flow cytometry

Apoptotic detection of siRNA-transfected cells was analyzed by staining cells with Annexin V-APC/7-amino-actinomycin D (7-AAD) (BD Biosciences, San Diego, CA, USA). Cell apoptotic rates (%) was determined as the sum of the 7AAA- annexin V+ population (% early apoptotic cells) and 7AAD+/ annexin V+ population (% late apoptotic cells). Cells were washed with PBS once prior to trypsinization with trypsin. The trypsinized cell pellet was gently resuspended in 1x binding buffer (BD Biosciences, San Diego, CA, USA). Subsequently, cells were stained by the addition of Annexin V-APC and 7-AAD. Cells were incubated in the dark for 10 min and subjected to detection by BD FACSCalibur flow cytometry (Becton Dickinson, San José, CA, USA). The apoptotic cell population was analyzed on the BD Cell Quest[®] version 3.3 (Becton Dickinson, San José, CA, USA) and WinMDI version 2.9 (The Scripps Research Institute, San Diego, CA, USA). All experiments were repeated at least 3 times.

Detection of cell cycle distribution using flow cytometry

Cell cycle distributions of siRNA-transfected cells were determined by flow cytometry DNA analysis. Cells were removed from plates by trypsin and fixed in 70% ethanol at -20 ° C. Fixed cells were washed with PBS and resuspended with 10 µg/ml ribonuclease A (Sigma-Aldrich, St. Louis, MO, USA) for 30 min. Resuspended cells were stained with 50 mg/mL propidium iodide (Sigma-Aldrich, St. Louis, MO, USA) for 15 min in the dark. DNA content was evaluated in BD Cell Quest® version 3.3 (Becton Dickinson, San José, CA, USA) and WinMDI version 2.9 (The Scripps Research Institute, San Diego, CA, USA). All experiments were repeated at least 3 times.

Gelatin invasion assay

The invasion ability of siRNA-transfected cells was observed using Transwell chambers with 8-µm pores size (Corning Inc., NY, USA). 1% gelatin with RPMI1640 was pipetted into the upper chamber (culture insert), which was placed in a lower chamber and dried on a clean bench. Cells transfected (1×10^5 cells/well) with siRNA with 0.2% bovine serum albumin were seeded in the upper chamber and then transferred to the lower chamber consisting of 400 µl 0.2% BSA medium containing human plasma fibronectin (Calbiochem, La Jolla, CA, USA). After overnight incubation at 37°C, the upper chamber was fixed with 70% ethanol and stained with Diff-Quik solution (Sysmex, Kobe, Japan). Nonmigrated cells on the inner surface of the upper chamber were wiped off using a cotton swab. Under an inverted microscope, invaded cells of the lower surface were then observed and counted in 5 selected fields under a light microscope. Results are expressed as mean \pm SD of the number of cells/field on three individual experiments.

Wound-Healing Assay

The wound-healing assay was subjected to Culture Inserts (Ibidi, Regensburg, Germany). Cells transfected with siRNA were seeded in Culture Inserts. After becoming confluent, the inserts were gently removed using sterile forceps. Next, cells were cultured with a new culture medium, and wound-healing was photographed at 3 random sites at 0, 24, and 48 h of culture. The gap distance for each hour was converted to 1 cm and statistically analyzed. All experiments were repeated at least 3 times.

Patients and tissue samples

Fresh CRC tissues and adjacent paired normal tissues were collected from 20 CRC patients who underwent colonoscopic biopsy at the Chonnam National University Hwasun Hospital (Jeonnam, Korea). Sera from 126 CRC patients who were histopathologically diagnosed in our hospital were obtained. CRC patients did not receive any therapy before serum and tissue sample collection and had no other severe systemic diseases. Sera from a healthy individual group were obtained from 126 healthy subjects who visited for routine health screening. The biopsy of the CRC tissues and adjacent normal tissues was quickly frozen in liquid nitrogen and stored at -80°C until the RNA was extracted. For immunohistochemistry, formalin-fixed and paraffin-embedded tissue samples were obtained from 425

patients who underwent surgery for pathologically confirmed colon cancers at the Chonnam National University Hwasun Hospital (Jeonnam, Korea) between July 2009 and June 2011. None of the patients had received preoperative radiotherapy or chemotherapy. The tissue blocks examined the original pathological slide, and the selected blocks showed the junction between the normal colonic epithelium and the tumor region. Tumor stages were performed according to the American Joint Committee on Cancer (AJCC) staging system (29). Overall survival was followed up on 31 December 2017 from the date of initiation of the operation. This study was approved by the Institutional Review Board (IRB No. CNUHH-2019-046) of the Chonnam National University Hwasun Hospital. Also, ethical approval was obtained from the Institutional Review Board of the Chonnam National University Hwasun Hospital. The biospecimens and data used for this study were provided by the Biobank of Chonnam National University Hwasun Hospital, a member of the Korea Biobank Network with the approval of IRB. All participants gave written consent for their information to be stored in the hospital database and used for research.

Enzyme-Linked Immunosorbent Assay (ELISA)

Blood samples were precipitated at room temperature for 30 min and centrifuged to separate serum. All serum samples were kept at -80°C before use. Serum levels of ELMO1 proteins were measured using ELMO1 ELISA kit (MyBioscience, San Diego, CA, USA), according to the manufacturer's instructions. Briefly, serum samples and standards are placed on a Microelisa plate. Next, HRP conjugate reagent was added to each well and incubated for 1 h at 37°C. After washing the plate 4 times, chromogen solution was added to the microplate, and the OD was determined using a microplate reader (Infinite M200; Tecan, Austria GmbH, Austria). Finally, OD values were converted to concentration using the standard curve derived from serially diluted ELMO1 standards. Each experiment was performed in triplicate wells.

Reverse transcription-polymerase chain reaction (RT-PCR)

Total RNA from siRNA-transfected cells was isolated using TRIzol reagent (Invitrogen, Carlsbad, CA, USA). After quantifying the amount of total RNA, 1 µg total RNA from each sample was converted to cDNA using 50 ng/µl oligo-dT and MMLV transcription reagents (Promega, Madison, WI, USA). Next, PCR amplification was performed using gene-specific primers and Go Taq[®] DNA polymerase (Promega, Madison, WI, USA). The sequences of the primers for ELMO1 were forward 5'-GCACTGAGCGATAACAGAAA-3' and reverse 5'-CCTGTCTTCCAGGAGGTTAAAG-3'. The sequences of the primers for GAPDH were forward 5'-ACCACAGTCCATGCCATCAC-3' / 5'-TCCACCACCCTGTTGCTGTA-3'. Finally, the PCR products were separated by electrophoresis on agarose gel and quantified on using Multi-Gauge software (ver 3.0, Fujifilm, Tokyo, Japan).

Immunohistochemistry

Paraffin-embedded sections (4-µm) were dewaxed and rehydrated with graded alcohols. Antigen recovery was carried out in citrate buffer (pH 6.0, Dako, Carpinteria, CA, USA) using a pressure cooker. The 10% goat serum and Dako REAL[™] peroxidase blocking solution (Dako) were then used to block endogenous antigen and endogenous peroxide activity, respectively. Sections were incubated with primary antibodies

against ELMO1 (Thermo, Rockford, IL, USA) at 1:600 dilution overnight at 4°C. TBST stained sections were stained using the Dako REAL™ Envision HRP/DAB detection system (Dako, Carpinteria, CA, USA) and counterstained with hematoxylin for 30 sec. Stained sections were observed and photographed using a light microscope.

Evaluation of ELMO1 expression

ELMO1 stained sections were divided into 2 groups (negative and positive) based on the percentage and intensity of stained cells. The percentage of stained cells was classified as follows: 0 (none), 1 (<10%), 2 (10-50%) and 3 (>50%). The degree of intensity of staining was classified as follows: 0 (no staining), 1 (weakly staining), 2 (moderately staining) and 3 (strongly staining). The overall score was defined as the value of the percent stain rating and intensity scores. The mean overall score of ≤ 3 was defined as negative, and of > 3 was defined as positive. All samples were evaluated by two independent observers without the knowledge of the patient clinical outcome data.

Statistical analysis

Statistical analysis was performed using statistical software the Statistical Package for Social Sciences (SPSS) software version 20.0 (IBM Corporation, Armonk, NY, USA). The relationship between ELMO1 expression and clinicopathological parameters was investigated using the Pearson Chi-square test. The diagnostic value of serum expression of ELMO1 was evaluated using receiver operating characteristic (ROC) analysis. Survival results were reported using the Kaplan-Merrier method, and the significance of the difference was confirmed using the logarithmic rank test. Univariate and multivariate analyses were done using Cox proportional hazards regression model. The results of the intergroup comparison were expressed as mean values \pm standard deviation (SD) of at least 3 independent experiments. The student's *t*-test was performed for the comparison of 2 groups. Significance was noted as $P < 0.05$.

Results

ELMO1 knockdown inhibits proliferation of human CRC cells

To investigate ELMO1 expression of ELMO1 in human CRC cells, the expression of the ELMO1 protein was examined by Western blotting in human CRC cell lines including DKO1, COLO205, HCT116, SW480 and DLD1. The expression of the ELMO1 protein was higher in SW480 and DLD1 cells among the cells tested (Fig. 1A). To investigate the function of ELMO1 in the oncogenic biologic behaviors of CRC cells, ELMO1 siRNA was used to knockdown endogenous expression of the ELMO1 gene in SW480 and DLD1 cells. ELMO1 protein expression showed a specific decrease by transfection of ELMO1 siRNA in SW480 and DLD1 cells (Fig. 1B). To access the potential of ELMO1 knockdown on cell proliferation, a cell proliferation assay was performed 1, 2, 3 and 4 days after transfection of the ELMO1 siRNA. ELMO1 siRNA-transfected SW480, and DLD1 cells significantly decreased the number of proliferating cells,

compared to siRNA-transfected scramble cells at 4 days, respectively ($P < 0.001$ and 0.007 , respectively) (Fig. 1C).

Elmo1 Knockdown Promotes Apoptosis Of Human Crc Cells

To evaluate whether ELMO1 knockdown could induce apoptosis, we performed flow cytometric analyzes. The cell apoptotic rate induced by transfection of ELMO1 siRNA increased significantly, compared to that induced by transfection of scramble siRNA in SW480 and DLD1 cells ($P = 0.028$ and 0.042 , respectively) (Fig. 2A, B). To determine caspase activation during ELMO1 knockdown-induced apoptosis, we further investigated caspase-specific activities. The expressions of cleaved caspase-3, -7 and PARP were significantly up-regulated in SW480 and DLD1 cells after ELMO1 knockdown (Fig. 2C). In addition, the level of anti-apoptotic Mcl-1 protein was significantly reduced by removing ELMO1 from SW480 and DLD1 cells (Fig. 2C).

ELMO1 knockdown induces cell cycle arrest of human CRC cells

To detect whether ELMO1 knockdown could change the distribution of the cell cycle, we performed flow cytometric analyzes. ELMO1 knockdown significantly promoted the apoptotic fraction (sub G1 phase) of SW480 and DLD1 cells ($P = 0.002$ and 0.022 , respectively) (Fig. 3A, B). Next, we evaluated the effects of ELMO1 on positive regulators, including cyclins, CDKs, and CDC25C in human CRC cells. As shown in Fig. 3C, the level of cyclin D1, CDK2, CDK4, CDK6 and CDC25C protein decreased significantly by the elimination of ELMO1 in SW480 and DLD1 cells.

ELMO1 knockdown inhibits the invasion and migration of human CRC cells

The number of SW480 and DLD1 cells invaded by transfected ELMO1 siRNA-transfected was significantly decreased compared to that of cells transfected with scramble siRNA ($P = 0.013$ and $P < 0.001$, respectively) (Fig. 4A). In addition, the artificial wound gap in the plates of cells transfected with scrambled siRNA became significantly narrower than in cells transfected with ELMO1 siRNA at 48 h in SW480 and DLD1 cells ($P < 0.001$ and $P = 0.010$, respectively) (Fig. 4B).

Elmo1 Knockdown Inhibits Emt In Human Crc Cells

To investigate the phenotypic changes induced by EMT in human CRC cells, the expression of well-known EMT associated target genes, such as E-cadherin, Vimentin and Claudin 1, was compared after transfection of scrambled siRNA and ELMO1 siRNA in SW480 and DLD1 cells. E-cadherin expression was significantly increased, and Vimentin and Claudin 1 significantly decreased in SW480 and DLD1 cells transfected with ELMO1 siRNA, compared to cells transfected with scramble siRNA (Fig. 5).

Impact of ELMO1 knockdown on oncogenic signaling pathways in human CRC cells

To explore the possible mechanisms of ELMO1 involved in the oncogenic behaviors of human CRC cells, we determined the phosphorylation levels of PDK1, Akt and GSK-3 β signaling proteins using Western blotting. The phosphorylation levels of PDK1, Akt, and GSK-3 β were significantly down-regulated by ELMO1 knockdown in SW480 and DLD1 cells (Fig. 6).

Expression of ELMO1 in cancer tissues and sera taken from human CRC patients

To confirm the results of the CRC cell line study, we evaluated the expression of ELMO1 at the RNA level by RT-PCR in 20 CRC tissues and the paired normal colon mucosa of the same patients taken by colonoscopic biopsy. We confirmed the up-regulation of ELMO1 expression in cancer tissues compared to paired normal mucosa at the mRNA level ($P=0.010$) (Fig. 7A). Additionally, we evaluated the expression of ELMO1 at the protein level by ELISA in sera taken from 126 CRC patients and 126 healthy individuals. The mean value of the ELMO1 protein in the sera of patients with CRC was significantly higher than that of healthy individuals ($P<0.001$) (Fig. 7B). Finally, ROC curve analysis was performed to explore whether serum expression of ELMO1 has diagnostic value in CRC. The results revealed that serum levels of ELMO1 could serve as a predictor for discriminating CRC patients from healthy individuals, with an AUC (the area under the ROC curve) of 0.803 (Fig. 7C). At the cutoff value of 3.790, the sensitivity and specificity were 71.4% and 71.4%, respectively.

Correlations between ELMO1 expression and clinicopathological characteristics in human CRC

To study the prognostic role of ELMO1 in the progression of human CRC, we investigated the immunohistochemical expression of the ELMO1 protein in formalin-fixed paraffin-embedded tissue blocks obtained from 425 CRC patients with clinicopathological data, including survival and the correlation between ELMO1 immunostaining and clinicopathological parameters was analyzed. Immunostaining of the ELMO1 protein was predominantly identified in the cytoplasm of cancer cells and was not detectable in the tumor stroma. On the contrary, immunostaining of the ELMO1 protein was not or was weakly stained in the normal colorectal mucosa (Fig. 8A, B). ELMO1 immunostaining was significantly associated with tumor stage, lymph node metastasis, and distant metastasis ($P<0.001$, $P<0.001$, and $P=0.002$, respectively) (Table 1). Furthermore, overall survival for patients with positive immunostaining for ELMO1 was significantly lower than that of patients without it ($P=0.014$) (Fig. 9). To evaluate the potential prognostic variables in patients with CRC, univariate and multivariate analyses using the Cox proportional hazard model were performed. In multivariate analysis, positive immunostaining of ELMO1 was independently associated with poor overall survival after adjustment of several covariates, such as age, sex, tumor size, lymphovascular invasion, perineural invasion, and cancer stage (Hazard ratio: 1.962; 95% CI: 1.345–2.861; $P<0.001$; Table 2).

Discussion

The ELMO protein family is a highly evolutionarily conserved protein family that plays a crucial role in cytoskeleton rearrangements during phagocytosis, cellular migration, chemotaxis, and metastasis of tumor cells (15–18). In mammals, the family of ELMO proteins consists of 3 ELMO genes, ELMO1,

ELMO2 and ELMO3 (8–15). Previously, ELMO3 expression was associated with tumor cell growth, invasion, metastasis, and a poor prognosis of colorectal cancer (26). However, the distinct function of ELMO1 in CRC remains to be explored.

Apoptosis is a programmed cell death that occurs regularly to control the tissue homeostatic balance between the rate of cell growth and cell death (30, 31). The cell cycle represents a series of strictly controlled fundamental events involving successive DNA replication and mitosis periods in cell biology (32, 33). However, dysregulation of apoptosis and cell cycle progression is the hall markers of cancer cells that can contribute to uncontrolled tumor cell growth and proliferation in many types of cancer (30–33). In our study, ELMO1 knockdown inhibited tumor cell proliferation, induced apoptosis and cell cycle arrest in human CRC cells. Therefore, ELMO1 expression can contribute to the progression of human CRC by dysregulating tumor cell survival and cell cycle progression. Previous studies showed that ELMO1 expression is associated with tumor cell growth, invasion and metastasis of variable human cancers including hepatocellular carcinoma, ovarian cancer, glioma, breast cancer, acute myeloid leukemia, and gastric cancer (20–25).

EMT is a critical process of cancer progression, by which epithelial cells lose cell-cell adhesion and transition to motile mesenchymal cells, and leads to an increase in migratory, invasive, and metastatic properties in cancer cells. (5–7). In our study, ELMO1 knockdown suppressed tumor cell invasion and migration, was associated with up-regulation of epithelial markers and down-regulation of mesenchymal markers in human CRC cells. Previously, ELMO1 expression was associated with EMT in human hepatocellular carcinoma and gastric cancer cells (18, 25), similar to our results.

To elucidate the underlying mechanisms that led to these results, we analyzed the effect of ELMO1 on the stimulation of multiple intracellular signaling pathways, which regulate the invasive and oncogenic phenotypes of human CRC cells. In our study, phosphorylation levels of Akt, GSK-3 β , and PDK1 were down-regulated by ELMO1 knockdown. Phosphoinositide-3-kinase/Akt (PI3K/Akt) and GSK-3 β are involved in a variety of cellular processes such as cell proliferation, differentiation, angiogenesis, cell cycle, and apoptosis. Additionally, they are the classical signaling pathways in tumorigenesis and influence the invasion, metastasis, and aggressiveness of cancer cells (34, 35). Previously, ELMO1 was associated with tumor cell progression through PI3K/Akt signaling in gastric cancer, hepatocellular carcinoma, and breast cancer (25, 36, 37). PDK1 is a master regulator of protein kinase A, G and C family kinases to control cell proliferation, apoptosis, and metabolic homeostasis and is considered the master upstream lipid kinase of the PI3K/Akt signaling pathway. PDK1 functions to phosphorylate and partially activate PI3K/Akt, triggering the activation of downstream effectors. Previously, PDK1 expression was up-regulated in multiple types of cancer and played a key role in cancer development and progression. Furthermore, PDK1 expression potentiates its downstream substrate PI3K/Akt to facilitate tumorigenesis (38, 39). Therefore, our results indicate that the alteration of PDK1 expression by ELMO1 may be a critical component of oncogenic PI3K/Akt signaling in human CRC.

ELMO1 expression has been reported to be highly expressed in various types of human cancers and has also been associated with tumor progression (20–25). Next, to confirm the results of the human CRC cell line study, we evaluated ELMO1 mRNA in human colorectal cancer tissues. We paired normal colorectal mucosa of the same patients taken by colonoscopic biopsy and the level of ELMO1 protein in sera taken from 139 CRC patients and healthy individuals, respectively. We confirm up-regulation of the level of ELMO1 mRNA in cancer tissues compared to paired normal mucosa in fresh colonoscopic biopsy specimens. Furthermore, the level of ELMO1 protein increased in sera from CRC patients compared to healthy individuals, suggesting its role as a diagnostic biomarker in CRC. These results suggest that ELMO1 has the potential to promote CRC development and progression. Further animal experiments are needed to evaluate the potential of ADAM12 as a diagnostic, prognosis, and therapeutic marker in CRC in the future.

Finally, we documented the expression of ELMO1 in a well-defined series of human CRCs, including long-term and complete follow-up, with special reference to the patient's prognosis. ELMO1 expression was significantly associated with tumor stage, lymph node metastasis, distant metastases, and poor survival. In addition, ELMO1 expression was independently associated with poor survival in multivariate analysis. These results suggest that ELMO1 expression may help predict the poor clinical outcome of human CRC.

Taken together, ELMO1 mediates tumor progression by increasing tumor cell motility and inhibiting apoptosis in human CRC.

Declarations

Ethics approval and consent to participate

Informed consent was obtained from all participants. This study was approved by the Institutional Review Board (IRB No. CNUHH-2019-046) of the Chonnam National University Hwasun Hospital. The study methodologies conformed to the standards set by the Declaration of Helsinki.

Consent for publication

Written informed consent was obtained from all participants, and their information was stored in the hospital database and used for research.

Availability of data and materials

All data generated or analyzed during this study are included in this published article.

Competing interests

The authors declare that they have no competing interests

Funding

This work was supported by the Korea National Research Foundation (NRF) grant funded by the Korea government (MSIT) (NRF-2017R1A2B-4004703 and NRF-2019R1F1A1063463), Republic of Korea.

Authors' contributions

YLP, SBC, DP and YEJ conceived and designed the present study. YLP, SBC, SYP and DP performed the experiments. HHO, EM, CMI, SS, SK, SYC, MWC, JYH, KHK, DSM and YEJ collected and analyzed the data. YLP, SBC, HHO and YEJ wrote, reviewed and/or revised the manuscript. WSL, DP confirmed the authenticity of all the raw data. All authors read and approved the final manuscript

Acknowledgements

Not applicable

References

1. Mattiuzzi C, Sanchis-Gomar F, Lippi G. Concise update on colorectal cancer epidemiology. *Ann Transl Med.* 2019 Nov;7(21):609.
2. Ahmed M. Colon Cancer: A Clinician's Perspective in 2019. *Gastroenterol Res.* 2020 Feb;13(1):1–10.
3. Jung G, Hernández-Illán E, Moreira L, Balaguer F, Goel A. Epigenetics of colorectal cancer: biomarker and therapeutic potential. *Nat Rev Gastroenterol Hepatol.* 2020 Feb;17(2):111–30.
4. Oh HH, Joo YE. Novel biomarkers for the diagnosis and prognosis of colorectal cancer. *Intest Res.* 2020 Apr;18(2):168–83.
5. Coban B, Bergonzini C, Zweemer AJ, Danen EH. Metastasis: crosstalk between tissue mechanics and tumour cell plasticity. *Br J Cancer.* 2021 Jan;124(1):49–57.
6. Majidpoor J, Mortezaee K. Steps in metastasis: an updated review. *Med Oncol.* 2021 Jan;38(1):3.
7. Datta A, Deng S, Gopal V, Yap KC, Halim CE, Lye ML, et al. Cytoskeletal Dynamics in Epithelial-Mesenchymal Transition: Insights into Therapeutic Targets for Cancer Metastasis. *Cancers (Basel).* 2021 Apr;13(8):1882.
8. Hochreiter-Hufford A, Ravichandran KS. Clearing the dead: apoptotic cell sensing, recognition, engulfment, and digestion. *Cold Spring Harb Perspect Biol.* 2013 Jan;5(1):a008748.
9. Brugnera E, Haney L, Grimsley C, Lu M, Walk SF, Tosello-Trampont AC, et al. Unconventional Rac-GEF activity is mediated through the Dock180-ELMO complex. *Nat Cell Biol.* 2002 Aug;4(8):574–82.
10. Lu M, Kinchen JM, Rossman KL, Grimsley C, deBakker C, Brugnera E, et al. PH domain of ELMO functions in trans to regulate Rac activation via Dock180. *Nat Struct Mol Biol* 11: 756-762, 2004. 11. Lu M, Kinchen JM, Rossman KL, Grimsley C, Hall M, Sondek J, Hengartner MO, Yajnik V and Ravichandran

- KS: A Steric-inhibition model for regulation of nucleotide exchange via the Dock180 family of GEFs. *Curr Biol.* 2005;15:371–7
11. Lu M, Kinchen JM, Rossman KL, Grimsley C, Hall M, Sondek J, et al. A Steric-inhibition model for regulation of nucleotide exchange via the Dock180 family of GEFs. *Curr Biol.* 2005 Feb;15(4):371–7.
 12. Gumienny TL, Brugnera E, Tosello-Tramont AC, Kinchen JM, Haney LB, Nishiwaki K, et al. CED-12/ELMO, a novel member of the Crkl/Dock180/Rac pathway, is required for phagocytosis and cell migration. *Cell.* 2001 Oct;107(1):27–41.
 13. Xu X, Jin T. ELMO proteins transduce G protein-coupled receptor signal to control reorganization of actin cytoskeleton in chemotaxis of eukaryotic cells. *Small GTPases.* 2019 Jul;10(4):271–9.
 14. Patel M, Margaron Y, Fradet N, Yang Q, Wilkes B, Bouvier M, et al. An evolutionarily conserved autoinhibitory molecular switch in ELMO proteins regulates Rac signaling. *Curr Biol.* 2010 Nov;20(22):2021–7.
 15. Patel M, Pelletier A, Côté JF. Opening up on ELMO regulation: new insights into the control of Rac signaling by the DOCK180/ELMO complex. *Small GTPases.* 2011 Sep;2(5):268–75.
 16. Abu-Thuraia A, Gauthier R, Chidiac R, Fukui Y, Screaton RA, Gratton JP, et al. Axl phosphorylates Elmo scaffold proteins to promote Rac activation and cell invasion. *Mol Cell Biol.* 2015 Jan;35(1):76–87.
 17. Michaelsen SR, Aslan D, Urup T, Poulsen HS, Grønbæk K, Broholm H, et al. DNA Methylation Levels of the ELMO Gene Promoter CpG Islands in Human Glioblastomas. *Int J Mol Sci.* 2018 Feb;19(3):E679.
 18. Peng H, Zhang Y, Zhou Z, Guo Y, Huang X, Westover KD, et al. Integrated analysis of ELMO1, serves as a link between tumour mutation burden and epithelial-mesenchymal transition in hepatocellular carcinoma. *EBioMedicine.* 2019 Aug;46:105–18.
 19. Wang Y, Xu X, Pan M, Jin T. ELMO1 Directly Interacts with G β Subunit to Transduce GPCR Signaling to Rac1 Activation in Chemotaxis. *J Cancer.* 2016 May;7(8):973–83.
 20. Jiang J, Liu G, Miao X, Hua S, Zhong D. Overexpression of engulfment and cell motility 1 promotes cell invasion and migration of hepatocellular carcinoma. *Exp Ther Med.* 2011 May;2(3):505–11.
 21. Wang J, Dai JM, Che YL, Gao YM, Peng HJ, Liu B, et al. Elmo1 helps dock180 to regulate Rac1 activity and cell migration of ovarian cancer. *Int J Gynecol Cancer.* 2014 Jun;24(5):844–50.
 22. Jarzynka MJ, Hu B, Hui KM, Bar-Joseph I, Gu W, Hirose T, et al. ELMO1 and Dock180, a bipartite Rac1 guanine nucleotide exchange factor, promote human glioma cell invasion. *Cancer Res.* 2007 Aug;67(15):7203–11.

23. Liang Y, Wang S, Zhang Y. Downregulation of Dock1 and Elmo1 suppresses the migration and invasion of triple-negative breast cancer epithelial cells through the RhoA/Rac1 pathway. *Oncol Lett.* 2018 Sep;16(3):3481–8.
24. Capala ME, Vellenga E, Schuringa JJ. ELMO1 is upregulated in AML CD34+ stem/progenitor cells, mediates chemotaxis and predicts poor prognosis in normal karyotype AML. *PLoS One.* 2014 Oct;9(10):e111568.
25. Park YL, Choi JH, Park SY, Oh HH, Kim DH, Seo YJ, et al. Engulfment and cell motility 1 promotes tumor progression via the modulation of tumor cell survival in gastric cancer. *Am J Transl Res.* 2020 Dec;12(12):7797–811.
26. Peng HY, Yu QF, Shen W, Guo CM, Li Z, Zhou XY, et al. Knockdown of ELMO3 Suppresses Growth, Invasion and Metastasis of Colorectal Cancer. *Int J Mol Sci.* 2016 Dec;17(12):E2119.
27. Hu Y, Yu Q, Zhong Y, Shen W, Zhou X, Liu X, et al. Silencing ELMO3 Inhibits the Growth, Invasion, and Metastasis of Gastric Cancer. *BioMed Res Int.* 2018 Sep;2018:3764032.
28. Pan C, Zhang Y, Meng Q, Dai G, Jiang Z, Bao H. Down Regulation of the Expression of ELMO3 by COX2 Inhibitor Suppresses Tumor Growth and Metastasis in Non-Small-Cell Lung Cancer. *Front Oncol.* 2019 May;9:363.
29. American Joint Committee on Cancer Classification (AJCC). *Cancer Staging Manual.* ed 6, revised. Philadelphia: Lippincott-Raven; 2002. pp. 113–23.
30. Obeng E. Apoptosis (programmed cell death) and its signals - A review. *Braz J Biol.* 2021 Oct-Dec;81(4):1133–43.
31. D’Arcy MS. Cell death: a review of the major forms of apoptosis, necrosis and autophagy. *Cell Biol Int.* 2019 Jun;43(6):582–92.
32. Liu J, Peng Y, Wei W: Cell cycle on the crossroad of tumorigenesis and cancer therapy. *Trends Cell Bio* S0962-8924: 00140-9, 2021.
33. Amoedo ND, El-Bacha T, Rodrigues MF, Rumjanek FD. Cell cycle and energy metabolism in tumor cells: strategies for drug therapy. *Recent Patents Anticancer Drug Discov.* 2011 Jan;6(1):15–25.
34. Bauer TM, Patel MR, Infante JR. Targeting PI3 kinase in cancer. *Pharmacol Ther.* 2015 Feb;146:53–60.
35. Luo J. Glycogen synthase kinase 3beta (GSK3beta) in tumorigenesis and cancer chemotherapy. *Cancer Lett.* 2009 Jan;273`2):194–200.

36. Peng H, Zhang Y, Zhou Z, Guo Y, Huang X, Westover KD, et al. Intergrated analysis of ELMO1, serves as a link between tumour mutation burden and epithelial-mesenchymal transition in hepatocellular carcinoma. EBioMedicine. 2019 Aug;46:105–18.

37. Erami Z, Khalil BD, Salloum G, Yao Y, LoPiccolo J, Shymanets A, et al. Rac1-stimulated macropinocytosis enhances Gβγ activation of PI3Kβ. Biochem J. 2017 Nov;474(23):3903–14.

38. Gagliardi PA, Puliafito A, Primo L. PDK1: at the crossroad of cancer signaling pathways. Semin Cancer Biol. 2018 Feb;48:27–35.

39. Atas E, Oberhuber M, Kenner L. The Implications of PDK1-4 on Tumor Energy Metabolism, Aggressiveness and Therapy Resistance. Front Oncol. 2020 Dec;10:583217.

Tables

Table I. Correlation between ELMO1 expression and clinicopathological parameters of human colorectal cancer

ELMO1; engulfment and cell motility 1

Table II. Cox regression analyses of the association between ELMO1 immunoreactivity and survival in human colorectal cancer adjusted for clinicopathological parameters

	Univariate analysis			Multivariate analysis		
	Hazard ratio	95% CI	p-value	Hazard ratio	95% CI	p-value
ELMO1 (negative vs. positive)	2.274	1.582-3.269	<0.001	1.962	1.345-2.861	<0.001
Age (<69.8 vs. ≥69.8 years)	1.301	0.912-1.857	0.147			
Sex (female vs. male)	0.878	0.614-1.254	0.473			
Tumor size (<4.9 vs. ≥4.9 cm)	1.377	0.975-1.945	0.069			
Lymphovascular invasion (negative vs. positive)	2.034	1.431-2.881	<0.001	1.596	1.091-2.334	0.016
Perineural invasion (negative vs. positive)	2.814	1.990-3.980	<0.001	2.278	1.572-3.300	<0.001
Stage (I/II vs. III/IV)	2.692	1.848-3.922	<0.001	1.723	1.136-2.613	0.010

Figures

Parameters	ELMO1			P-value
	Total (n =425)	Negative (n =215)	Positive (n =210)	
Age (years)				0.166
<69.8	184	86	98	
≥69.8	241	129	112	
Sex				0.198
Male	254	135	119	
Female	171	80	91	
Tumor size (cm)				0.943
<4.9	232	117	115	
≥4.9	193	98	95	
Histologic type				0.556
Well Differentiated	185	98	87	
Moderately differentiated	193	97	96	
Poorly differentiated	32	13	19	
Mucinous and signet ring cell	15	7	8	
Lymphovascular invasion				0.123
Negative	300	159	141	
Positive	125	56	69	
Perineural invasion				0.266
Negative	298	156	142	
Positive	127	59	68	
Stage				<0.001
I	59	39	20	
II	147	94	53	
III	181	72	109	
IV	38	10	28	
Depth of invasion (T)				

T1	20	15	5	0.102
T2	59	32	27	
T3	324	159	165	
T4	22	9	13	
Lymph node metastasis (N)				<0.001
N0	214	137	77	
N1-3	211	78	133	
Distant metastasis (M)				0.002
M0	365	197	168	
M1	60	18	42	

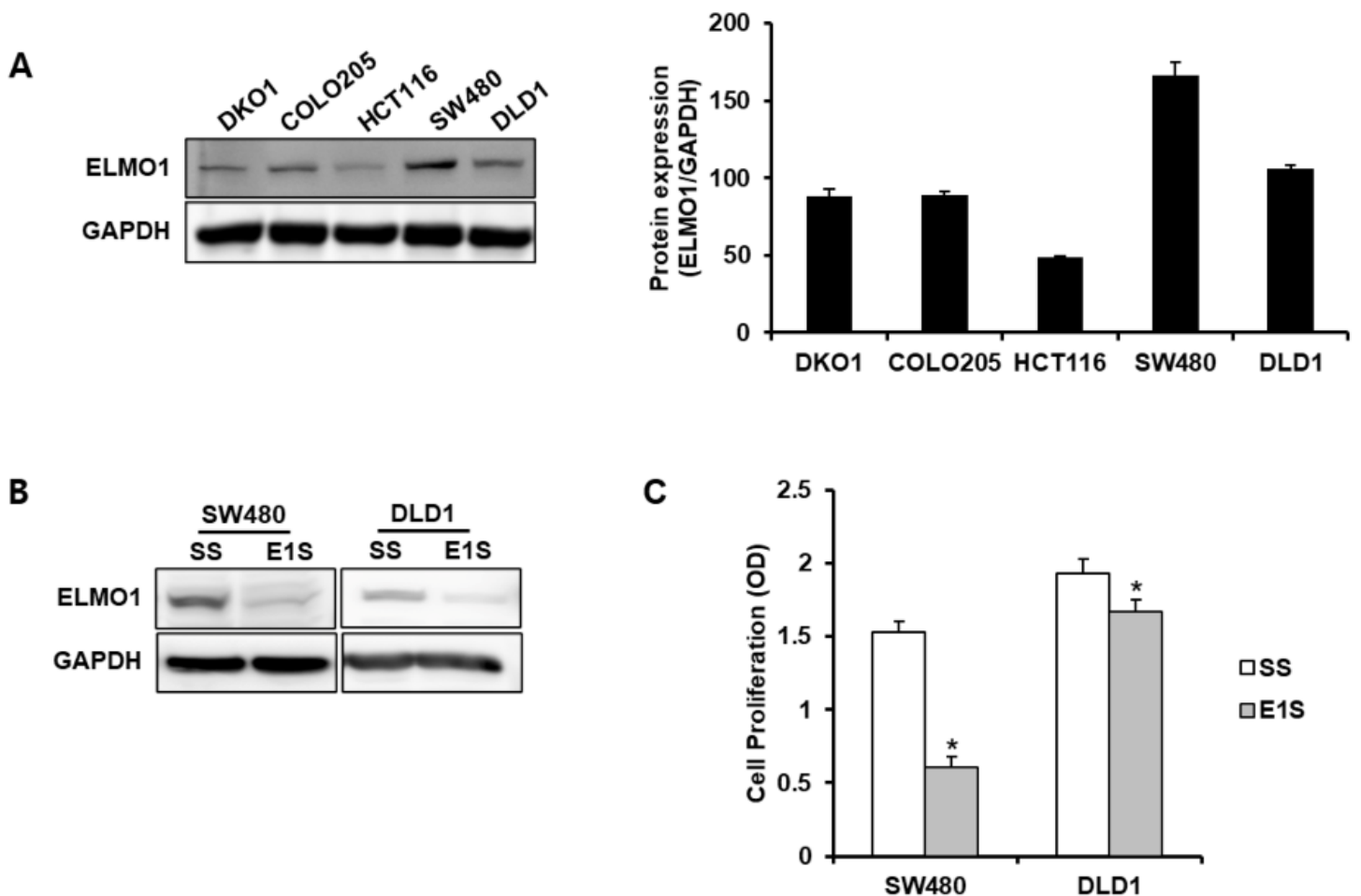


Figure 1

ELMO1 knockdown inhibits proliferation of human CRC cells. (A) Expression of the ELMO1 protein in human CRC cell lines. Graphical representation of band intensities was quantified using the Multi-gauge gel analysis software. (B) Effect of ELMO1 knockdown in human CRC cells. Expression of the ELMO1

protein was decreased by transfection of E1S into SW480 and DLD1 cells. (C) Impact of ELMO1 knockdown on the proliferation of human CRC cells. E1S-transfected SW480 and DLD1 cells significantly decreased the number of proliferating cells, compared to cells transfected with SS at 4 days, respectively (mean±SD, n=3; **P* < 0.05). ELMO1; engulfment and cell motility 1, CRC; colorectal cancer, SS; scramble siRNA, E1S; ELMO1 siRNA, SD; standard deviation.

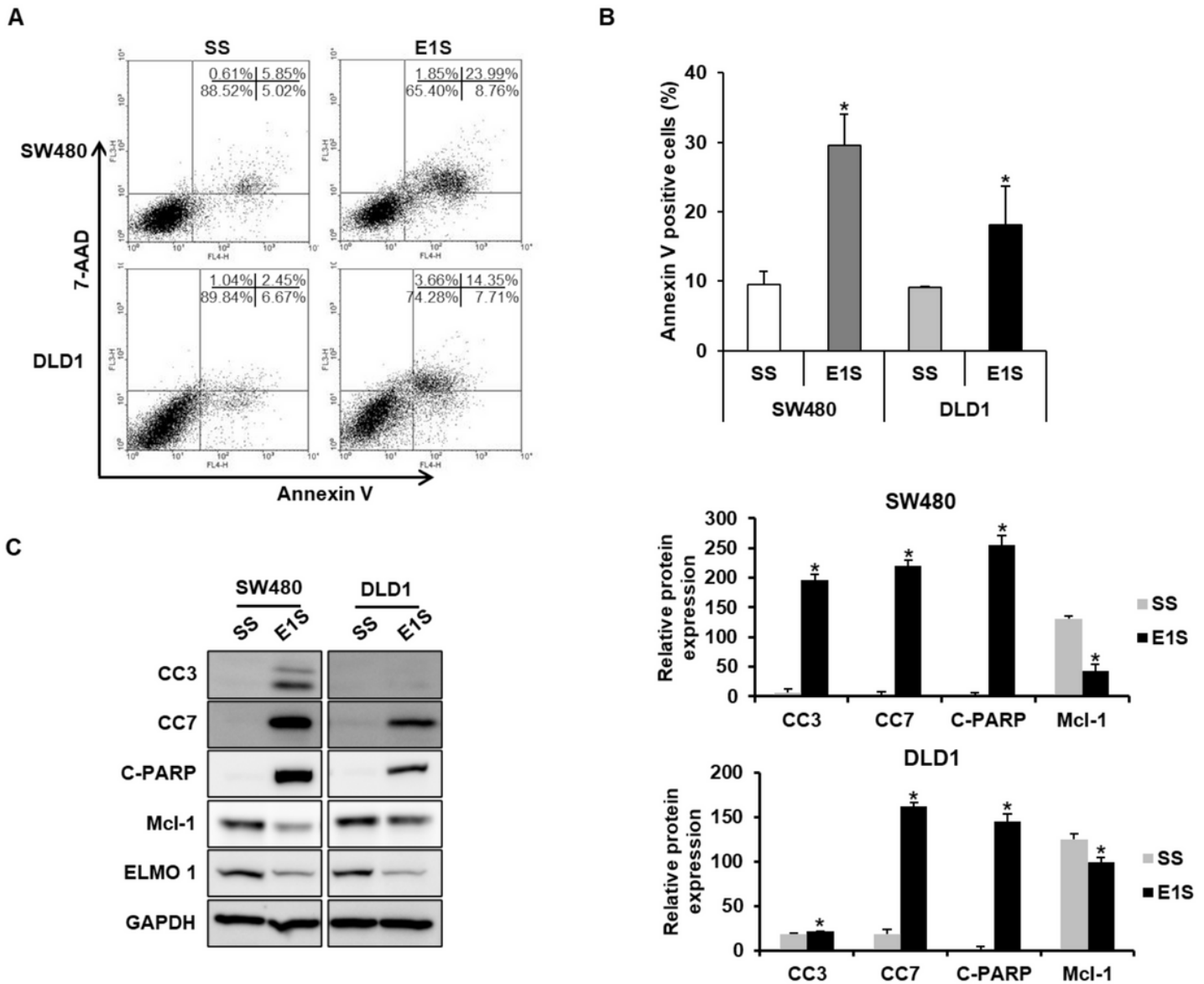


Figure 2

ELMO1 knockdown promotes apoptosis of human CRC cells. (A) Representative flow cytometry plots. One representative experiment from the three independent experiments is shown. (B) The proportion of apoptotic cells induced by E1S transfection was greater than that induced by SS transfection in SW480 and DLD1 cells (mean±SD, n=3; **P* < 0.05). (C) Expression of the cleaved caspase-3, -7, PARP, and Mcl-1 proteins. The cleaved caspase-3, -7 and PARP expressions were up-regulated and anti-apoptotic Mcl-1 protein level was down-regulated in the SW480 and DLD1 cells after ELMO1 knockdown. Each bar represents the mean ± SD of 3 experiments. **P* < 0.05 versus scrambled siRNA-transfected cells. ELMO1;

engulfment and cell motility 1, CRC; colorectal cancer, SS; scramble siRNA, E1S; ELMO1 siRNA, PARP; poly (ADP-ribose) polymerase, Mcl-1; myeloid cell leukemia-1, SD; standard deviation.

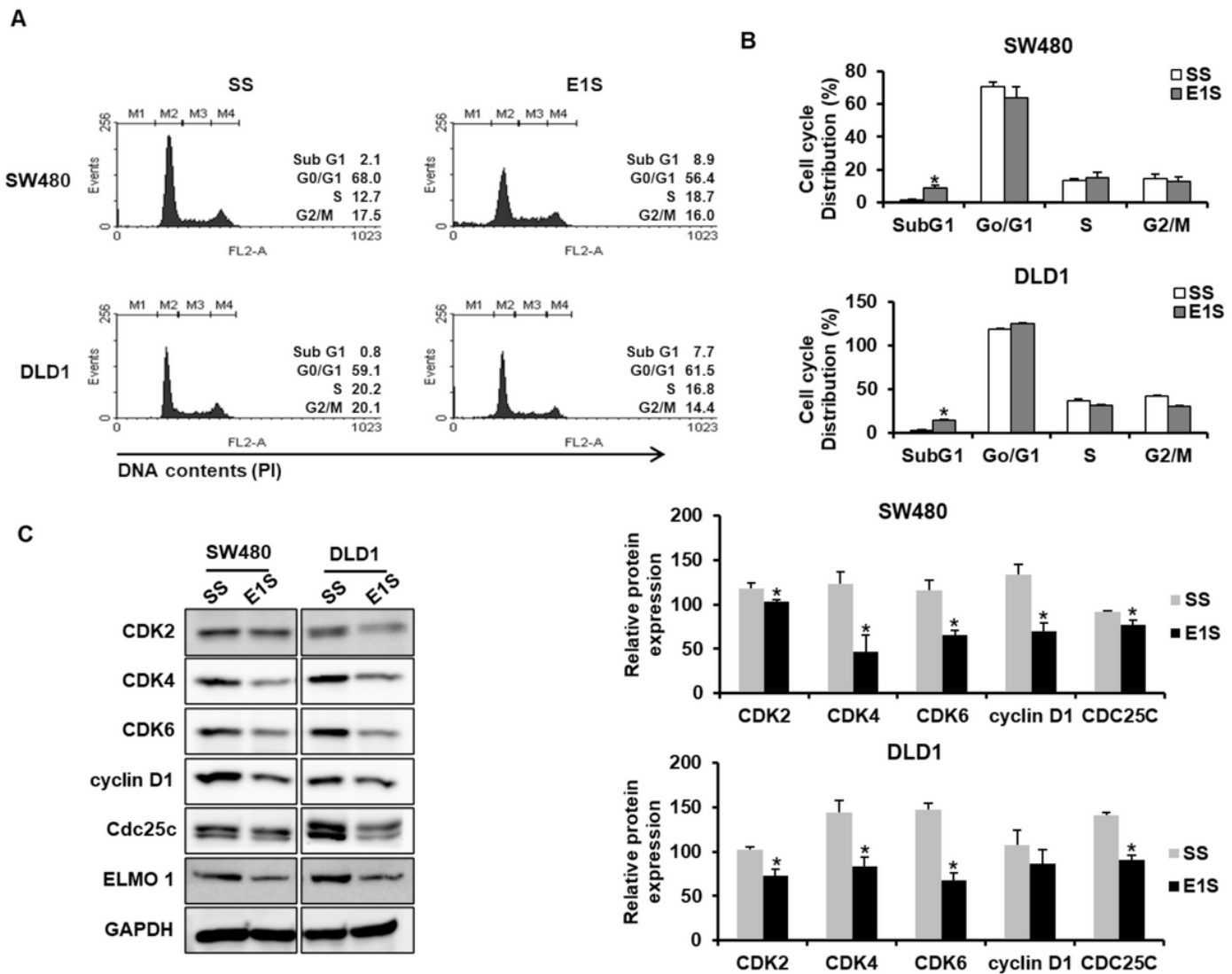


Figure 3

ELMO1 knockdown induces cell cycle arrest of human CRC cells. (A) Representative flow cytometry plots. One representative experiment from the three independent experiments is shown. (B) ELMO1 knockdown significantly promoted the apoptotic fraction (sub G1 phase) of SW480 and DLD1 cells (mean \pm SD, n=3; * P < 0.05). (C) Expression of cell cycle regulatory proteins. The level of cyclin D1, CDK2, CDK4, CDK6, and CDC25C protein decreased significantly by ELMO1 knockdown in SW480 and DLD1 cells. Each bar represents the mean \pm SD of 3 experiments. * P < 0.05 versus scrambled siRNA-transfected cells. ELMO1 knockdown. ELMO1; engulfment and cell motility 1, CRC; colorectal cancer, SS; scramble siRNA, E1S; ELMO1 siRNA, CDK; cyclin-dependent kinase, CDC25C; cell division cycle 25C, SD; standard deviation.

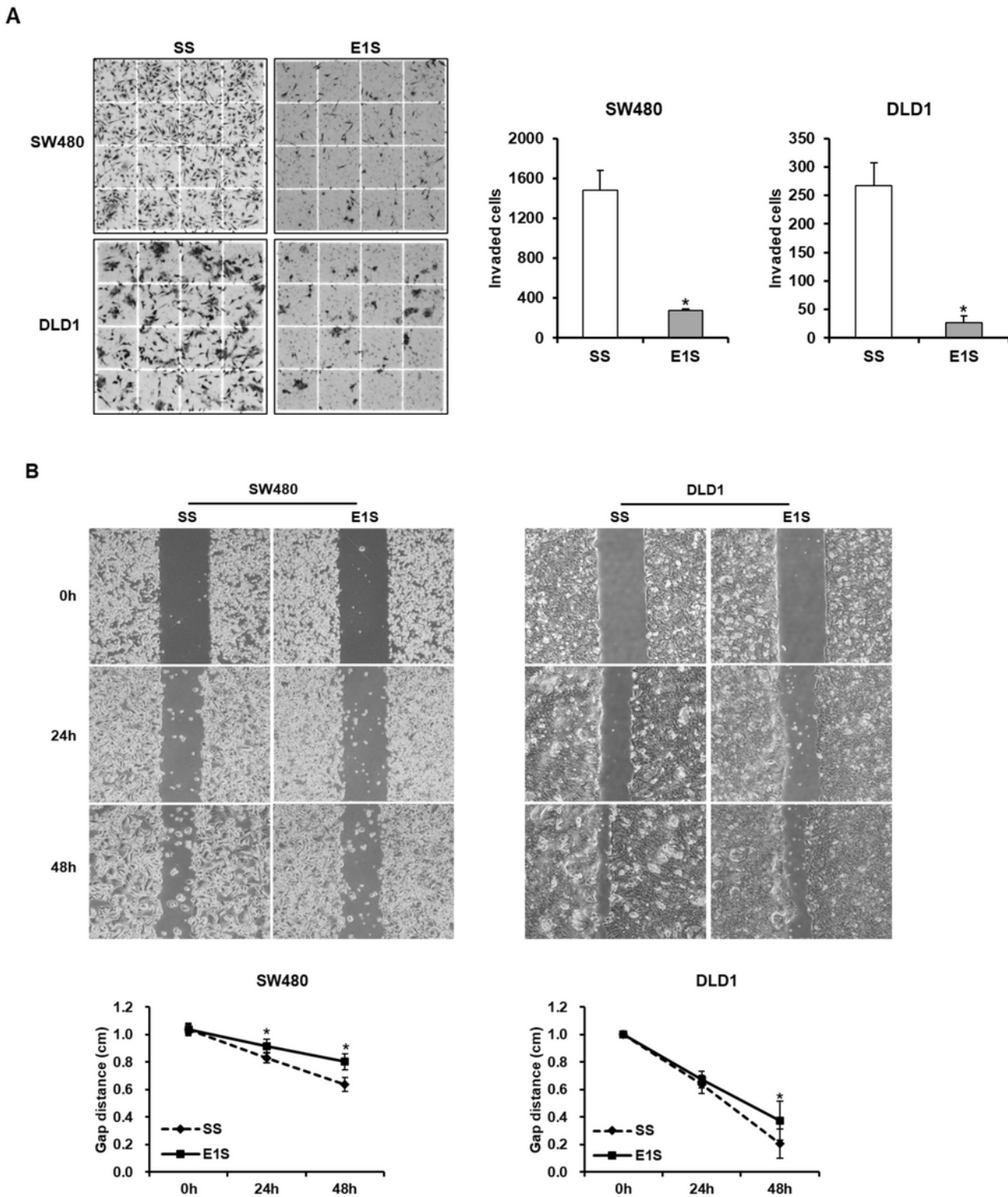


Figure 4

ELMO1 knockdown inhibits invasion and migration of human CRC cells. (A) Impact of ELMO1 knockdown on the invasion of human CRC cells. Invasion assay was performed using siRNA-transfected cells. The stained invading cells were counted and are represented as graphs between groups. The number of cells invaded was significantly lower than in cells (mean±SD, n=3; * $P < 0.05$). (B) Impact of ELMO1 knockdown on human CRC cell migration. The wound healing assay is performed using siRNA-

transfected cells and cell migration graphs are displayed as relative healing distances (mean±SD, n=3; **P* < 0.05). The artificial wound gap in plates of SS-transfected cells became significantly narrower than in E1S-transfected cells at 48 h in SW480 and DLD1 cells. ELMO1; engulfment and cell motility 1, CRC; colorectal cancer, SS; scramble siRNA, E1S; ELMO1 siRNA, SD; standard deviation.

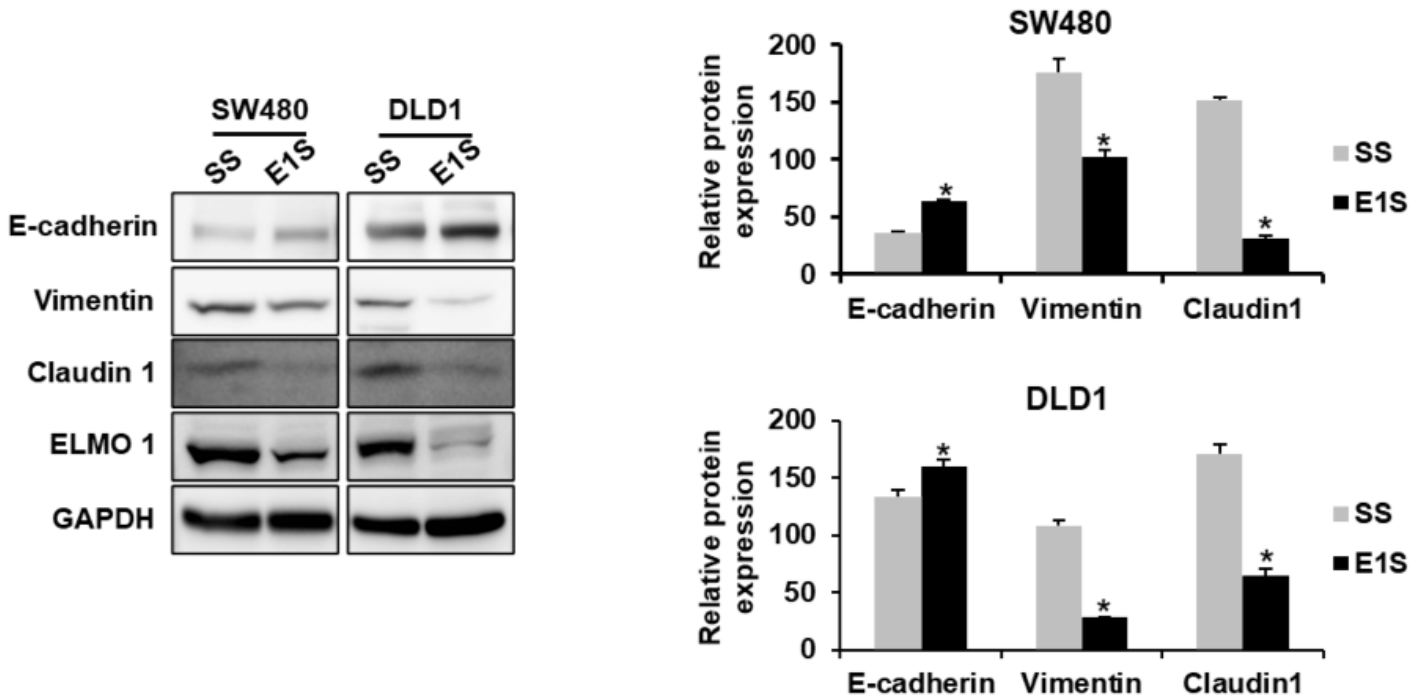


Figure 5

ELMO1 knockdown inhibits EMT in human CRC cells. Impact of ELMO1 knockdown on the EMT of human CRC cells. The expression of E-cadherin increased and Vimentin and Claudin 1 decreased in SW480 and DLD1 cells transfected with E1S, compared to SS-transfected cells. Each bar represents the mean ± SD of 3 experiments. **P* < 0.05 versus scrambled siRNA-transfected cells. ELMO1; engulfment and cell motility 1, CRC; colorectal cancer, SS; scramble siRNA, E1S; ELMO1 siRNA, EMT; epithelial-mesenchymal transition, SD; standard deviation.

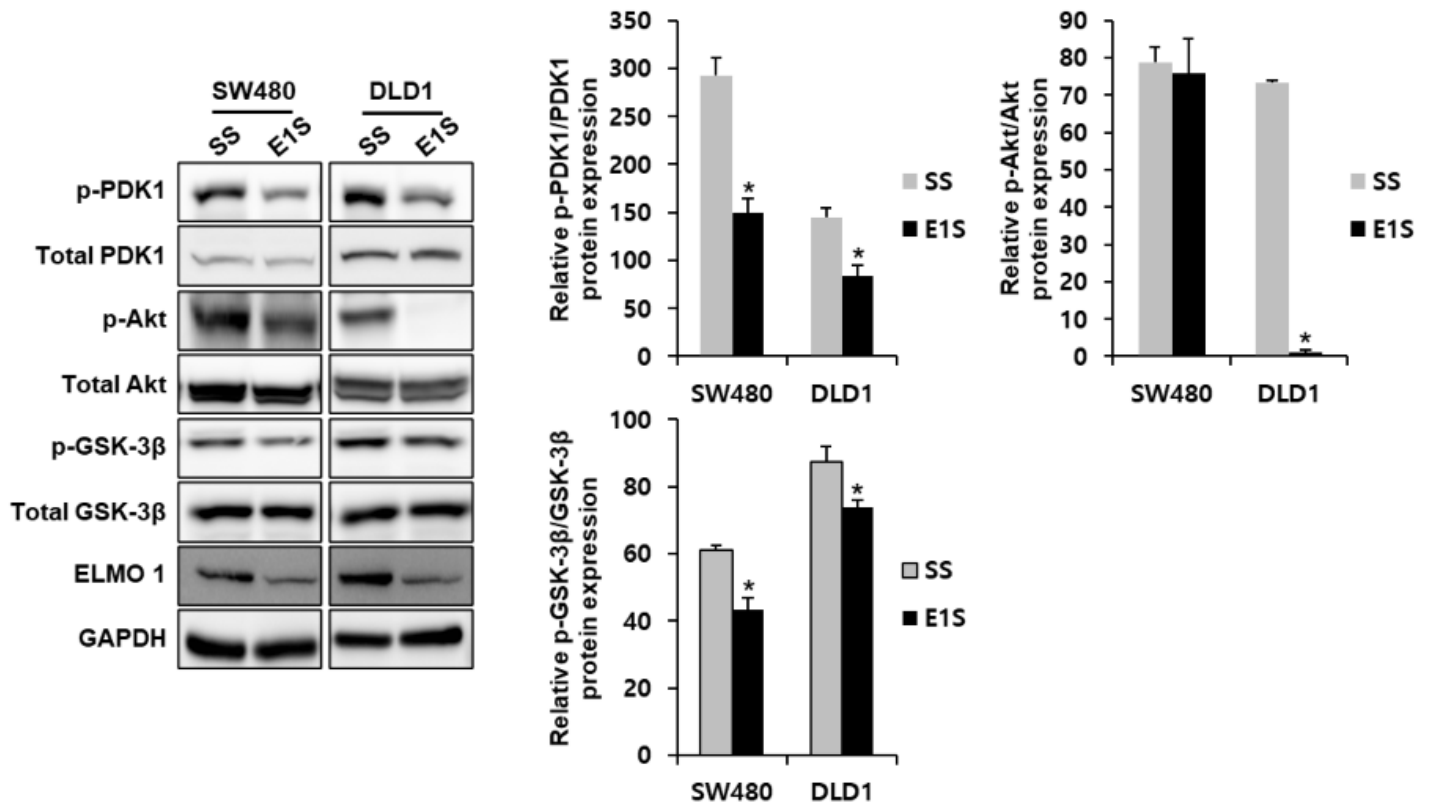


Figure 6

Impact of ELMO1 knockdown on oncogenic signaling pathways in human CRC cells. The phosphorylation levels of Akt, GSK-3 β , and PDK1 were down-regulated by ELMO1 knockdown in SW480 and DLD1 cells. Each bar represents the mean \pm SD of 3 experiments. * $P < 0.05$ versus scrambled siRNA-transfected cells. ELMO1; engulfment and cell motility 1, CRC; colorectal cancer, SS; scramble siRNA, E1S; ELMO1 siRNA, GSK-3 β ; glycogen synthase kinase 3 β , PDK1; phosphoinositide-dependent protein kinase 1, SD; standard deviation.

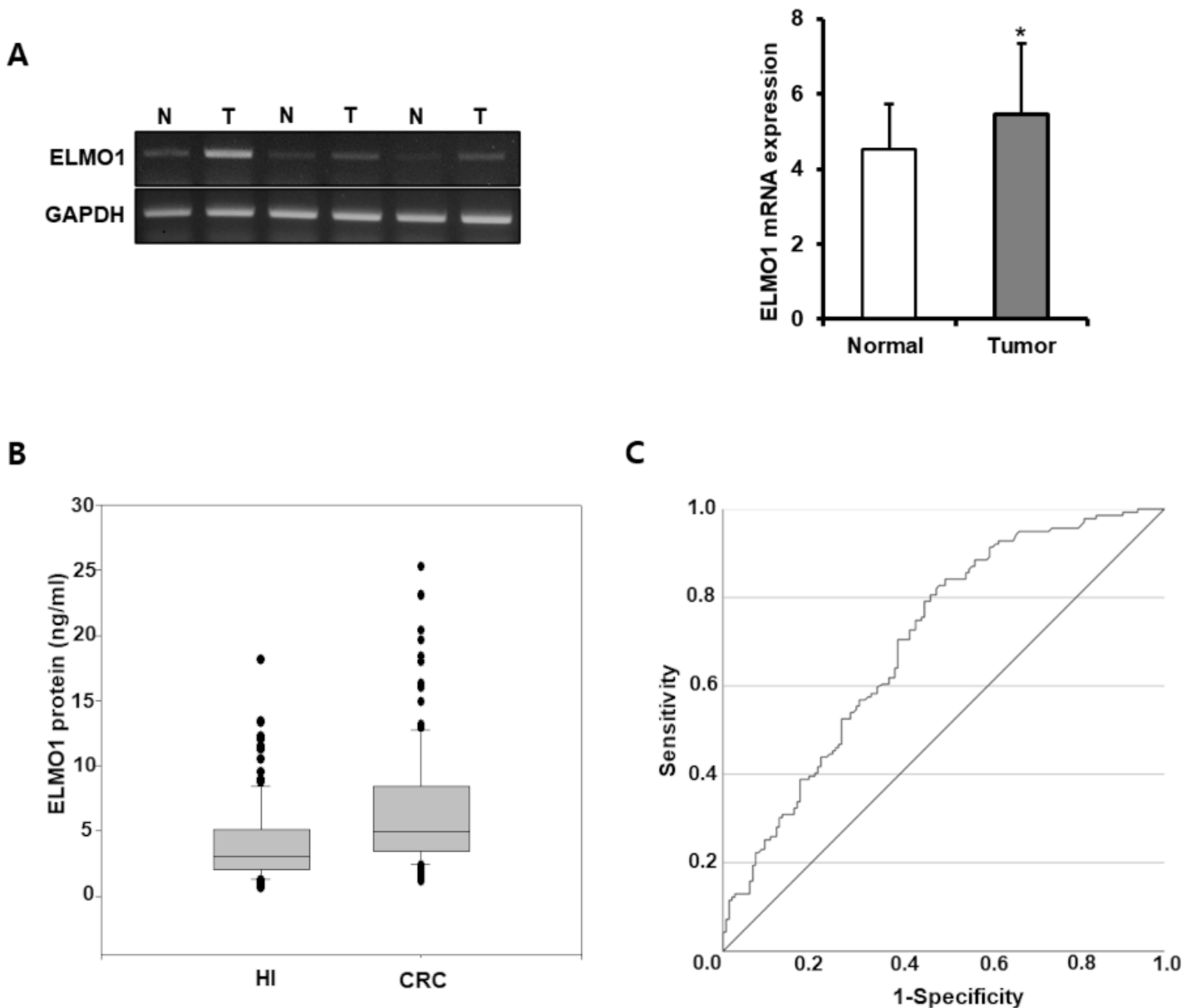


Figure 7

Expression of ELMO1 in colonoscopic biopsy samples and sera by RT-PCR and ELISA. (A) ELMO1 expression is up-regulated in cancer tissues compared to the normal mucosa paired at the mRNA level in colonoscopic biopsy specimens. Each bar represents the mean \pm SD of 20 cases. * $P < 0.05$ versus normal colonic mucosa. (B) ELMO1 expression at the protein level was evaluated by ELISA in sera taken from 126 CRC patients and 126 healthy individuals. The mean value of the ELMO1 protein in the sera of CRC patients was significantly higher than in healthy individuals. * $P < 0.05$ versus healthy individuals. (C) Analysis of the ROC curve for the detection of CRC using ELMO1 serum. At the cutoff value of 3.790, the sensitivity and specificity were 71.4% and 71.4%, respectively. AUC = 0.803. ELMO1; engulfment and cell motility 1, RT-PCR; reverse transcription-polymerase chain reaction, ELISA; enzyme-linked immunosorbent assay, ROC; receiver operating characteristic, T; colorectal cancer tissue, N; paired normal colonic mucosa, HI; healthy individuals, CRC; colorectal cancer patient, SD; standard deviation, AUC; area under curve.

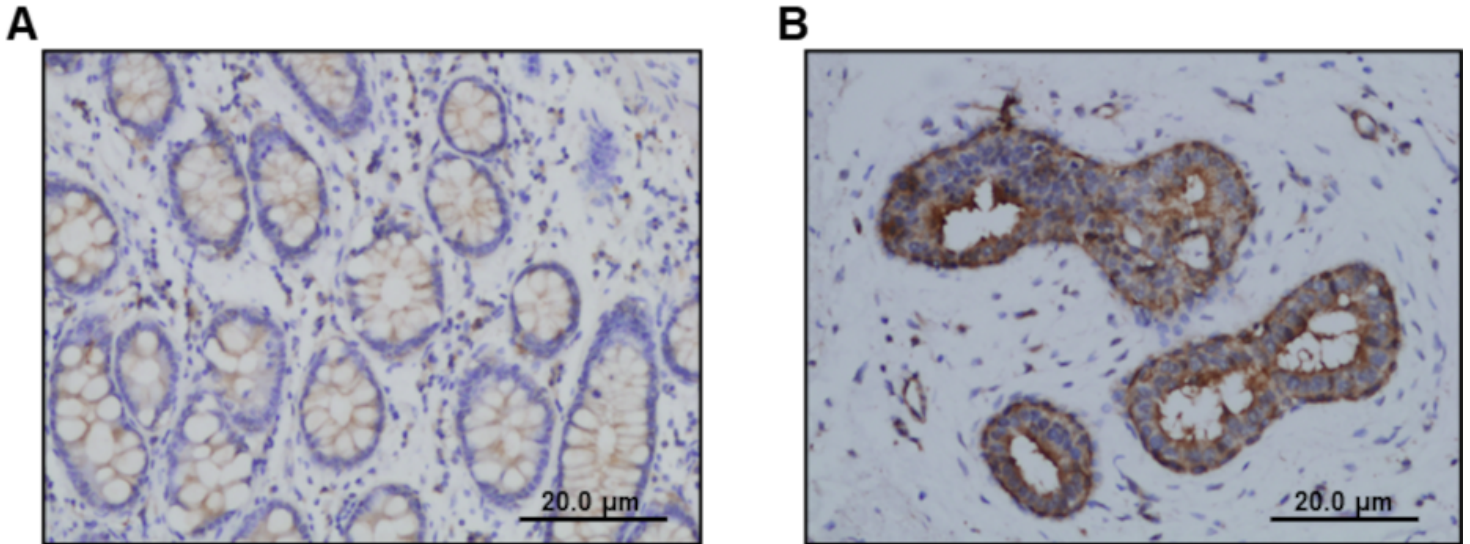


Figure 8

Expression of ELMO1 in human CRC tissues by immunohistochemistry. (A) Immunostaining of the ELMO1 protein was not or weakly stained in the normal colorectal mucosa (x200). (B) Immunostaining of the ELMO1 protein was predominantly identified in the cytoplasm of cancer cells and was not detectable in the tumor stroma (x200). CRC; colorectal cancer, ELMO1; engulfment and cell motility 1.

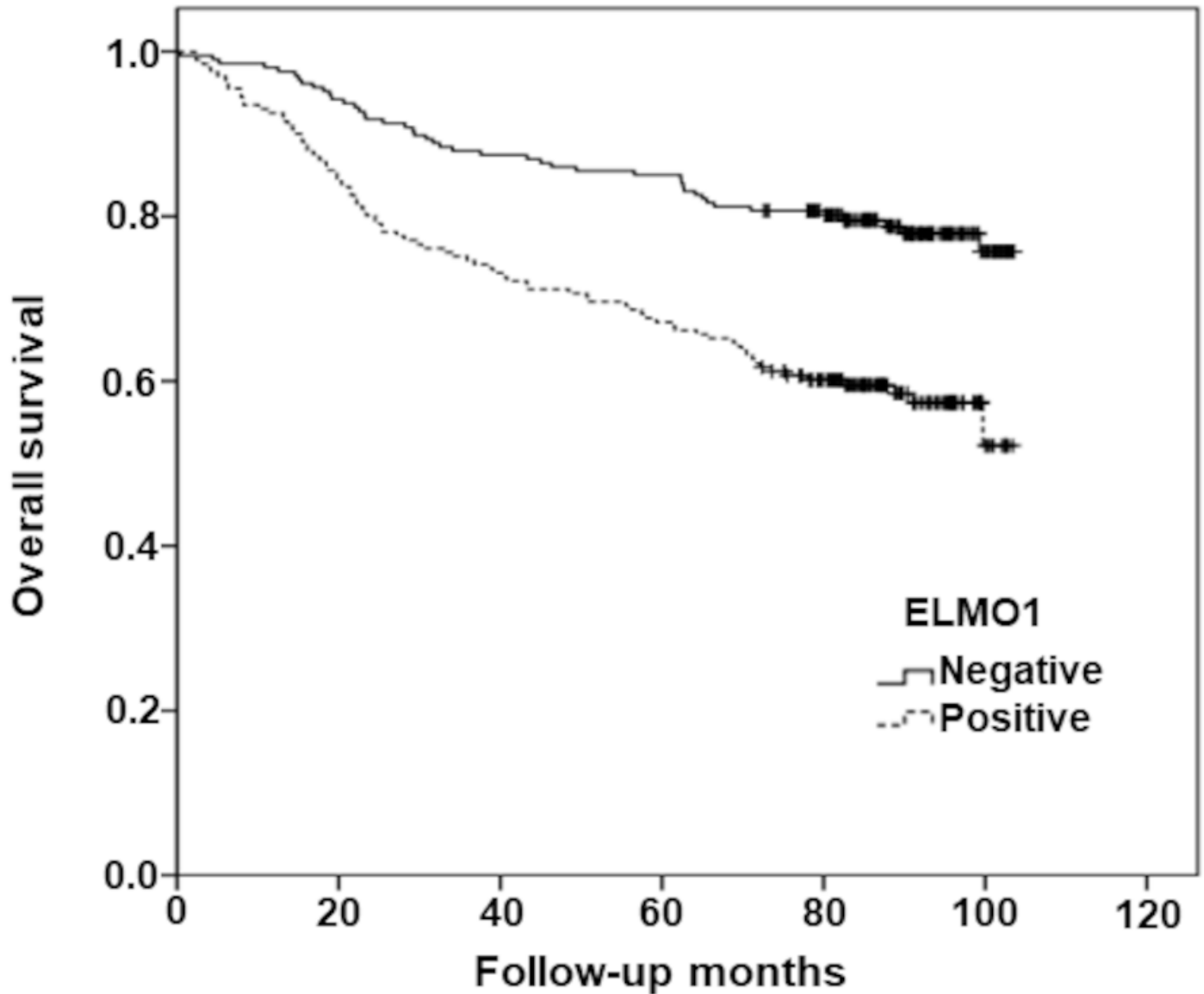


Figure 9

Kaplan-Meier survival curve correlating overall survival with positive expression (solid line) and negative expression (dotted line) of ELMO1. Overall survival for patients with positive immunostaining for ELMO1 was significantly lower than that of patients without it ($P = 0.014$). ELMO1; engulfment and cell motility 1.

Supplementary Files

This is a list of supplementary files associated with this preprint. Click to download.

- [Supplementarydata.pdf](#)